ELSEVIER

Nuclear Instruments and Methods in Physics Research A 449 (2000) 322–330

NUCLEAR INSTRUMENTS & METHODS IN PHYSICS RESEARCH Section A

www.elsevier.nl/locate/nima

Neutron time-of-flight measurement techniques: new possibilities of TOF spectroscopy with NEAT at BENSC

B. Rufflé[1], J. Ollivier, S. Longeville[2], R.E. Lechner*

Hahn-Meitner-Institut, Abt. NI, Glienicker Str. 100, D-14109 Berlin, Germany

Raeceived 11 October 1999; received in revised form 18 November 1999; accepted 2 December 1999

Abstract

A series of experiments performed on the TOF spectrometer NEAT at the Berlin Neutron Scattering Center is reported to demonstrate the versatility and some of the original possibilities offered by this instrument: continuous variation of the energy resolution over four decades, TOF diffraction using single detectors and a large range of incident neutron wavelengths, high-resolution studies in (Q, ω)-space of single crystals with a multidetector at large scattering angle, or elastic and inelastic small-angle scattering with the multidetector at zero angle.

PACS: 61.12.-q; 61.12.Ex; 61.12.Yp; 87.80. + s

Keywords: Neutron instruments; Time of flight; Resolution; Quasielastic scattering; Inelastic small-angle scattering; TOF diffraction

1. Introduction

NEAT is a high-resolution multichopper time-of-flight spectrometer for inelastic neutron scattering experiments in the region of medium to very small energy and momentum transfers, including elastic and inelastic small angle scattering experiments. Due to the optimized design of the instrument [1,2], the data rate of NEAT in standard operation with its single detectors [3,4] is very comparable to that of the ILL spectrometer IN5, in spite of the much lower flux of the BER-II reactor. While a number of results from NEAT in standard operation, concerning studies of atomic and molecular motions in ion conducting plastic crystals [5–7], superionic glasses [8], ternary glass systems [9–11], soft matter [12], proteins and biological membranes [13–17], as well as spin dynamics in high-T_c superconductors [18–20], have already been published, several less conventional possibilities of this spectrometer have been explored only recently. The present paper focuses on measurement–technical aspects of such original experiments that have now become feasible with NEAT. We demonstrate this with the aid of four examples. In Section 2, a brief description of the TOF spectrometer NEAT will be given. Section 3 presents typical spectra that can be obtained with the single detector bank in standard operation allowing to measure the dynamical behaviour with an energy resolution, which can be continuously varied over four decades. In Section 4, the TOF-diffraction capacity of NEAT with a large range of incident

* Corresponding author. Tel.: + 49-30-8062-2780; fax: + 49-30-8062-2181.

E-mail address: lechner@hmi.de (R.E. Lechner).

[1] Now at Laboratoire Des Verres, UMR 5587 CNRS, Université Montpellier II, F-34095 Montpellier, France.

[2] Now at Laboratoire Léon Brillouin, CE Saclay, F-91191 Gif/Yvette, France.

0168-9002/00/$ - see front matter
PII: S0168-9002(99)01370-4

neutron wavelengths is demonstrated. Section 5 shows the very first quasielastic spectra from a single crystal, measured with high (Q *and* ω)-resolution, using the NEAT multidetector at a large scattering angle. In Section 6, the elastic and inelastic small-angle scattering option with the multidetector of NEAT at zero angle will be presented.

2. Instrument description

The TOF monochromator of NEAT (Fig. 1) is a chopper cascade which produces a pulsed monochromatic neutron beam by means of seven phased disk choppers with magnetic bearings (CH(1,2) to CH(6,7)). The time and energy widths of the neutron pulses are variable in large ranges via the variation of three independent technical parameters: the chopper speed, the chopper window widths, and the chopper phases; the latter are used to define the neutron wavelength. Higher resolution corresponds to larger chopper speeds, narrower chopper windows, and/or longer neutron wavelengths. The divergence and the cross-section of the incident beam are controlled by a beam exchanger (SW) permitting the optional use of a diaphragm system for small-angle scattering experiments, and of a supermirror-coated double-trumpet guide section for large-angle scattering. NEAT is equipped with an array of 388 ^{3}He single detectors (SD) at fixed distance (2.50 m) from the sample, for large-angle scattering, and a two-dimensional position-sensitive ^{3}He detector (multidetector or MD) at variable distance (4–7.30 m) from the sample, for small-angle scattering. Furthermore, the multidetector can also be used for large-angle scattering in the same range of distances and in the whole angular range of the SDs (see Fig. 1). This permits an appreciable increase of energy and momentum resolution to be obtained in regions of the solid angle selected by the user.

3. Standard operation with the SD

One of the most essential properties of NEAT is the high flexibility of its chopper system. The chopper speed range of 750–20 000 rpm, the possibility of using different chopper window widths and the incident neutron wavelength range of 2–16 Å allow to vary continuously the energy resolution of quasielastic neutron scattering experiments between 4 μeV and 10 meV, i.e. over 4 orders of magnitude. (Note, that still longer wavelengths are available in principle, but not included in this range, because of insufficient flux for most experiments employing energy analysis.) This instrument is especially suitable for studies of complex systems such as disordered crystals, glasses, molecular liquids and solutions, soft matter, and biological samples. For instance, it is well known that the large number of polypeptide side groups and other molecular subunits as part of biological complexes and their individual motions are responsible for an enormous variety in the dynamical behaviour of these materials. The faster stochastic molecular motions (time scale: 10^{-7}–10^{-13} s) are made visible using neutron spectroscopy. To study the characteristics of these motions in a wide range of correlation times, one has to carry out measurements at many different energy resolutions. Such an opportunity is now available using one and the same instrument, namely NEAT. As an example, spectra of purple membrane (PM) that had been equilibrated at 98% relative humidity (D_2O), were measured [21] with five different energy resolutions ($\Delta E = 1000$, 300, 100, 34 and 10 μeV (FWHM)). Three of these are shown in Figs. 2a–c as obtained with the different incident wavelengths $\lambda = 4.54$, 5.1 and 6.2 Å. The essentially elastic vanadium spectra representing the resolution function are also shown. The three PM spectra, in spite of identical dynamics, show strong quasielastic components with rather different apparent linewidths. This is due to the well-known phenomenon of preferential observation of excitations just outside the elastic resolution window in quasielastic neutron scattering, where slower motions are hidden within the "elastic" component, and faster motions are buried in the "inelastic background". This example clearly shows the occurrence of stochastic motions in biological macromolecules ranging at least from nanoseconds to a few tenth of picoseconds and the necessity to obtain data at many different energy resolutions, which is an easy task for NEAT. Note that, even with one single incident neutron

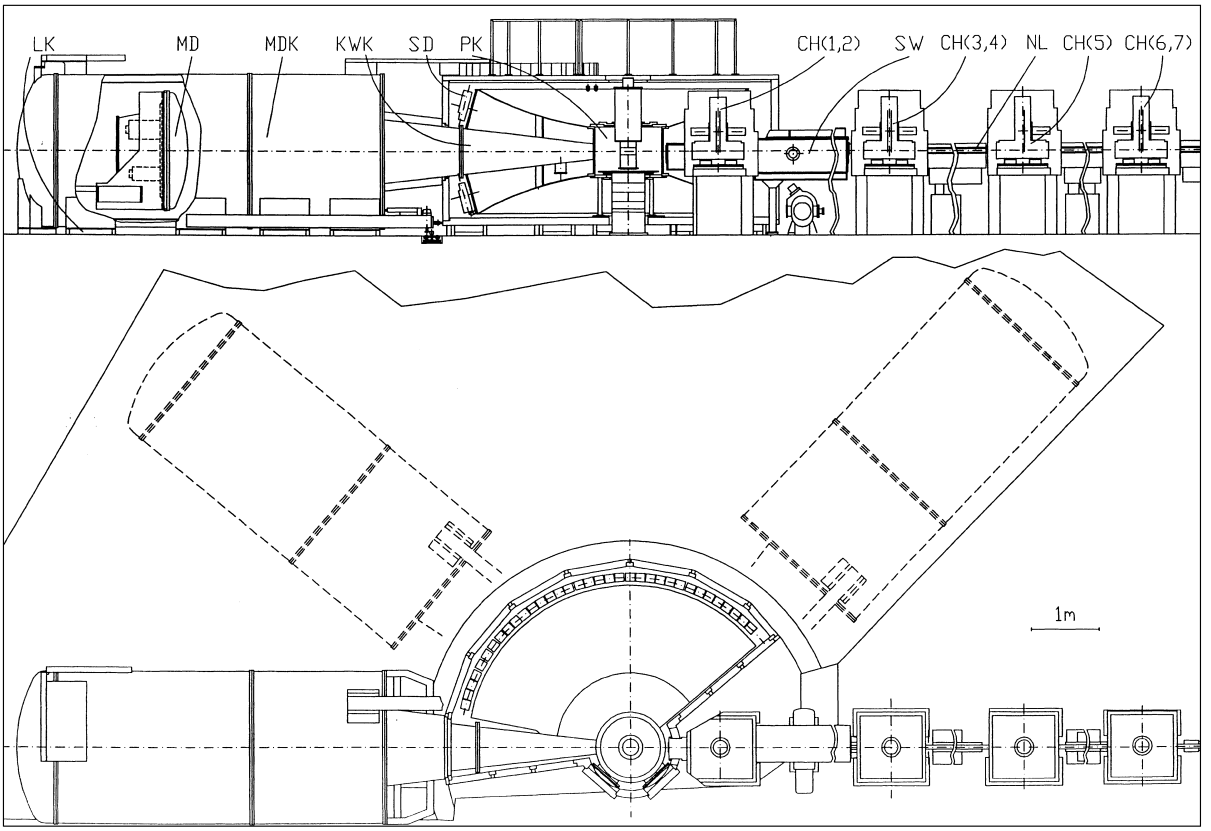

Fig. 1. Sketch of the time-of-flight spectrometer NEAT. The sample is mounted in the "PK" chamber and receives the incident pulsed beam monochromatized by the seven chopper disks "CH 1-7". The scattered neutrons are counted by the single detector array "SD" at a fixed distance of 2.50 m from the sample, at scattering angles between 13.3° and 136.7°, and by the multidetector "MD", at a distance between 4 m and 7.3 m from the sample in the "MDK" chamber. Furthermore, the "MDK" chamber, mounted on air pads, can be moved towards large angles up to 120°. Since the total length of the spectrometer (23 m) could not be accommodated in the figure, a large part of the neutron guide sections (in between choppers) has been omitted.

wavelength, it is possible to obtain spectra with very different energy resolutions. For example, a ratio of about 1:40 between highest and lowest energy resolution ($\Delta E = 56$ and 2280 μeV, respectively) is achieved at $\lambda = 5.1$ Å with NEAT using the single detectors. A further extension of the lower limit (to $\Delta E = 26$ μeV at this wavelength) and the ratio 1:88 is achieved, when the multidetector is employed at its largest distance from the sample.

4. TOF diffraction experiments

If only the last pair of counter rotating choppers is used at low speed, a pulsed "white" beam is produced which permits time-of-flight diffraction experiments [22,23] to be carried out. The chopper speed and the duration of the period have been chosen to allow the recording of TOF diffraction patterns with the single detectors, with neutron wavelengths from 1 to 20 Å. Fig. 3 presents a typical TOF diffraction spectrum, measured with NEAT. The sample studied was the so-called muscovite "amber" mica at $T = 10$ K, which belongs to the layered alumino-silicate structural family. The known value of its d_1-spacing (9.926 Å) [24] has been used to calibrate precisely the TOF scale in units of wavelength for this configuration. As an example demonstrating the use of a large wavelength range, and especially of long

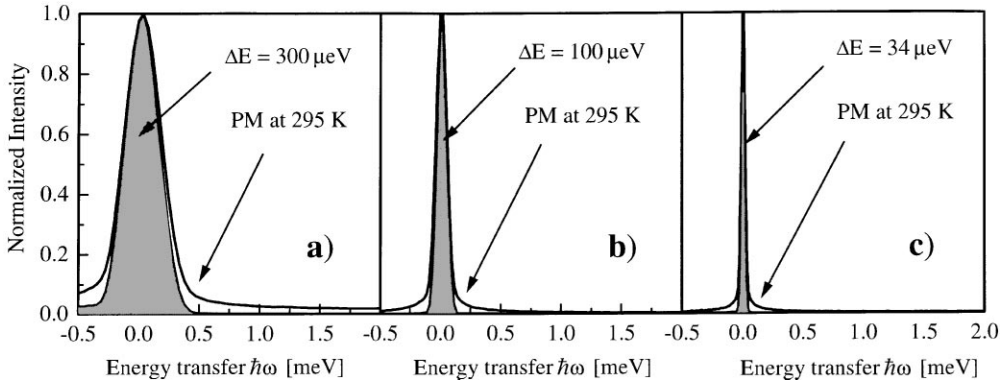

Fig. 2. Purple membrane spectra measured with three different energy resolutions ((a) 300, (b) 100 and (c) 34 μeV (FWHM)) using incident wavelengths $\lambda = 4.54$, 5.1 and 6.2 Å. The shaded spectra represent the resolution function obtained from a vanadium standard sample. In spite of identical dynamics the three PM spectra show strong quasielastic components with rather different apparent linewidths. Sample: stacks of purple membrane equilibrated at 98% relative humidity (D_2O), at room temperature. Illuminated sample size: (30×60) mm^2. Measurement times: 3 h ($\Delta E = 300$ μeV), 7 h ($\Delta E = 100$ μeV) and 14.4 h ($\Delta E = 34$ μeV), respectively.

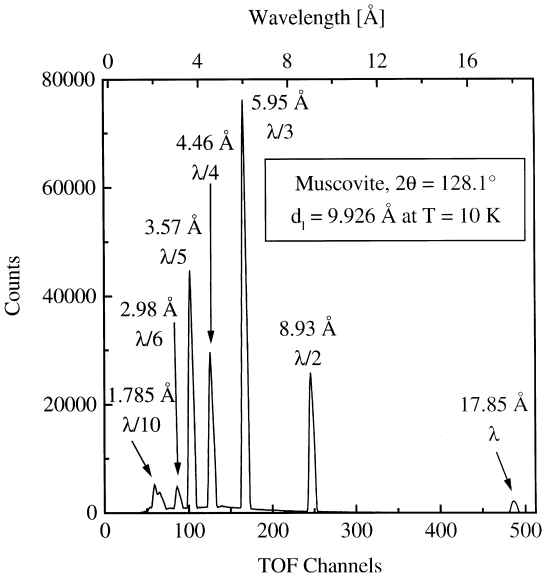

Fig. 3. TOF diffraction pattern of a layered alumino-silicate structure (muscovite, $d_1 = 9.926$ Å), measured with NEAT at $T = 10$ K, showing well defined reflections up to incident neutron wavelengths of 17.85 Å. These reflections have been used to calibrate precisely the TOF scale in units of wavelength. Illuminated sample size: 12 mm diameter. Measurement time: 2.5 h.

wavelengths, which are very suitable for studies of samples with large unit cells, we have carried out a series of experiments on purple membrane multilayer systems. Lamellar reflections up to the fifth order have been measured simultaneously at low scattering angles at room temperature. Four of them are shown together in Fig. 4 for the scattering angle $2\theta = 22.7°$, for a PM sample equilibrated in the presence of D_2O vapour at 98% relative humidity (r.h.). This leads to a very precise determination of the lamellar spacing constant d_1, when all the data are analyzed simultaneously, as shown in the inset of Fig. 4. Note that the lamellar reflections are seen in a relatively large 2θ-range because of the appreciable mosaic spread (FWHM = 12°) of the oriented PM stacks [25]. Furthermore in principle, the intense first-order lamellar reflection, which has been observed simultaneously at a much lower angle in the first single detector ($2\theta = 13.5°$), could also have been measured together with the four others at $2\theta = 22.7°$, with a period of twice the length actually used, allowing slower neutrons with wavelengths up to 40 Å to be recorded, without frame overlap. It is also interesting to note that this technique takes advantage of the "inverse" order in which the lamellar reflections are measured on the wavelength scale: high orders (low intensity) are observed with short wavelengths (high flux), and low orders (high intensity) with long wavelengths (low flux), thus allowing the simultaneous observation of all the reflections with reasonable statistical accuracy. The most important point, however, is obviously, that this crucial structural information can be unambiguously related to the dynamical

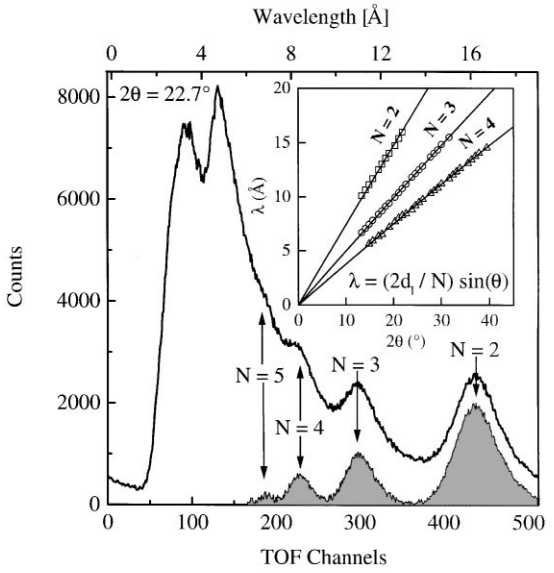

Fig. 4. TOF diffraction pattern of a PM multi-layer stack equilibrated at 98% relative humidity (D_2O), measured at room temperature with NEAT, exhibiting four orders of lamellar reflections at $2\theta = 22.7°$. The inset shows the result of a simultaneous refinement of three orders of lamellar reflections, which leads to an accurate determination of the lamellar spacing constant, $d_l = 85.6 \pm 0.2$ Å. For clarity, the shaded surface shows the TOF-diffraction pattern, where the incoherent background has been subtracted. It was however not corrected for the incident flux distribution, in order to keep – for the purpose of presentation – the intensities of the different reflections at comparable levels. Illuminated sample size: (30×60) mm^2. Measurement time: 2.8 h.

one, as standard inelastic scattering experiments can follow immediately on the same spectrometer, without removing the sample from the cryostat.

5. High (Q, ω)-resolution with the MD at large-scattering angle

One of the main novelties offered by the TOF spectrometer NEAT is the (64×64)-channel position-sensitive detector, which can be used to increase significantly the energy and momentum resolutions at any scattering angle selected by the user. This very new possibility in TOF spectroscopy has been used recently to analyse the low-frequency critical dynamics around a commensurate-incommensurate displacive phase transition in a molecular compound [26]. Bis 4-Chloro-Phenyl Sulfone (BCPS) is a monoclinic crystal (I2/a), which undergoes at $T_I = 150$ K a second-order phase transition towards a modulated incommensurate structure existing down to the lowest temperature investigated (at least down to 6 K). In previous experiments, this transition was found to be characterized by the softening and – within the approximation applied to this pre-transitional dynamic phenomenon – by the saturation at $\omega(q_s, T_I) = 78 \pm 4$ GHz $(322 \pm 16$ μeV) of an optic mode inside the Brillouin zone and the growing of an unresolved central peak component at the satellite position $q_s = 0.78\boldsymbol{b}^*$ [27]. The dynamical character of this central peak is still a matter of debate and it has been the aim of the experiment reported here to determine the energy width of this component. To go beyond the results obtained with triple-axis spectrometers, we used the multidetector option of the time-of-flight spectrometer NEAT to significantly improve the energy resolution, keeping a very good wave-vector resolution, needed to observe this kind of critical dynamics in single crystals. With an incident wavelength set to 6.8 Å, the chopper speed to 20 000 rpm, and the multidetector located at 7.23 m from the sample position, a resolution of 13.6 μeV (FWHM) has been achieved at zero energy transfer, where a MD cell covers 0.92×10^{-6} Å^{-2}. At this wavelength, the scattering angle 2θ corresponding to the satellite peak Q_s (4 0.78 0) was roughly 120°, where the multidetector was put. Fig. 5a shows a contour plot of the time-of-flight integrated intensity measured on the MD around the satellite position at $T = T_I + 1$ K. The pre-transitional diffuse scattering is better seen in Fig. 5b which is a cut along the $\boldsymbol{b}^*$-axis corresponding to the horizontal line through the peak centre in Fig. 5a. At this temperature, the width of the diffuse scattering is completely consistent with what has been previously observed in this compound by triple-axis spectrometry. But the most interesting feature is the low-energy dynamical behaviour in the neighbourhood of this Bragg satellite position at Q_s. Fig. 6 clearly shows a quasielastic broadening of the central peak (obtained from a limited summation of spectra in the neighbourhood of the satellite position, see legend of the figure) in this molecular crystal by

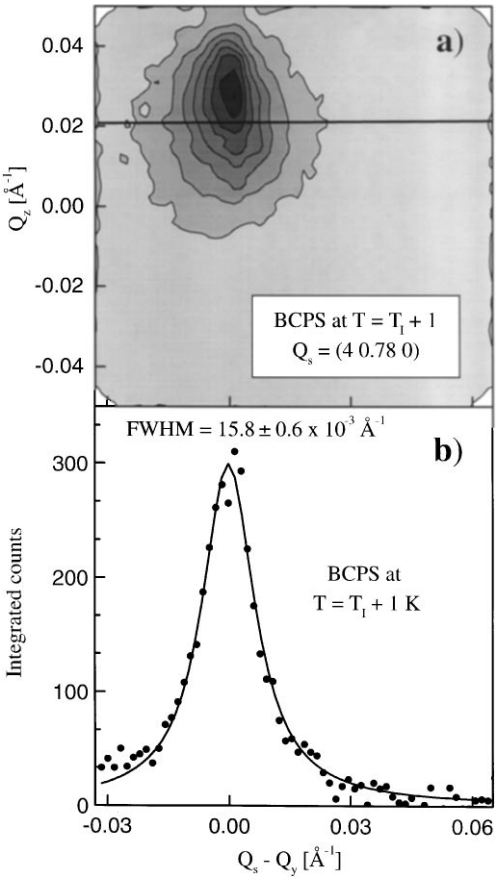

Fig. 5. (a) Central peak at the satellite position Q_s of the molecular crystal BCPS at $T = T_1 + 1$ K, measured with the MD (TOF channels integrated). (b) Diffuse scattering along $\boldsymbol{b}^*$ (horizontal cut through the maximum in Fig. 5a). Illuminated sample size: (10×20) mm^2 (roughly cylindrical crystal, 20 mm high). Measurement time: 19 h.

comparison with a vanadium spectrum which is purely elastic in this energy window. This quasielastic broadening was not seen during previous triple-axis spectrometer experiments, where the best resolution width was, at least, 10 times larger than the one achieved with NEAT. Note that this component cannot be associated with the condensed soft mode, because at this temperature and in this energy window, the latter appears as a flat background. This very first observation gives an idea of the potential of such a method for experiments with very high resolution in Q and ω, which

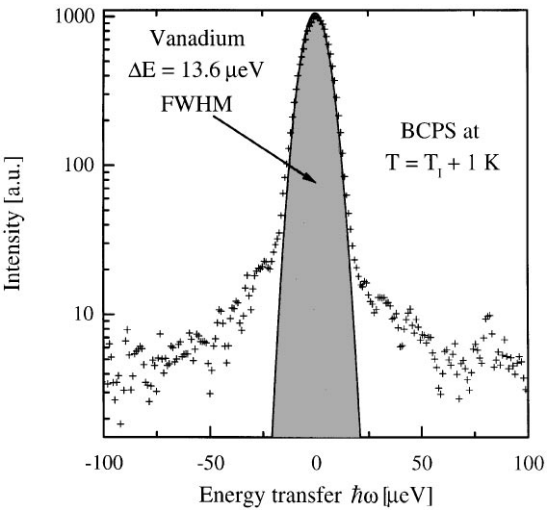

Fig. 6. Energy analysis of the TOF spectrum of Fig. 5 around Q_s at the same temperature, integrated over (9×13) MD-elements (corresponding to a rectangular surface of 1.07×10^{-4} Å^{-2} with the long side along the z-direction), centered at the satellite peak. This clearly shows a quasielastic broadening of the central peak. Measurement time: 19 h.

are sometimes needed to answer unresolved questions in condensed matter physics.

6. Elastic and inelastic small-angle scattering

More recently the elastic and inelastic small-angle scattering option of NEAT has been tested successfully. The multidetector chamber has been put at the zero angle position, whereas the sample-multidetector distance has been set to 4 m. After replacing the supermirror-coated "double-trumpet" guide section by the diaphragm system, in order to achieve the beam collimation required for small-angle scattering experiments, we have measured the well-known structure factor of a porous silica glass (CPG-10-75) with $\lambda = 6$ Å (Fig. 7), which is very similar to what is found in the literature [28]. After this first crucial test, we have undertaken a series of inelastic small-angle scattering experiments, with different energy resolutions, on a solution of lysozyme in D_2O (66 mg/ml, $pD = 3.6$), with $\lambda = 3.5$ Å. Fig. 8a shows a contour plot of the diffraction pattern of the solution obtained on the MD at room temperature and Fig. 8b

presents the energy-integrated (continuous line) and the elastic (open circles) structure factors of lysozyme in solution deduced from Fig. 8a after removing the D_2O contribution. Because of the energy analysis performed, the measurement times (see legends of Figs. 7 and 8) are obviously much longer than in the case of conventional SANS instruments. It is also clear, that small-angle scattering diffraction patterns could be measured much more efficiently with the TOF-diffraction technique (see Section 4) employing a large band of incident neutron wavelengths. We are, however, not trying to compete with static SANS experiments here: the main interest of the kind of experiment presented, is shown in Figs. 8b and c. In the latter a complete inelastic small-angle TOF spectrum of the solution (resolution: $\Delta E = 261$ μeV) taken at $Q = 0.128$ Å^{-1}, integrated over an annulus of 6.8×10^{-3} Å^{-1} width, is shown. This allows to separate the very narrow and intense elastic peak (maximum value: 155 in the arbitrary units of the figure) from the broad inelastic contribution, which together give rise to the structure factors of such globular proteins, as measured in conventional small-angle scattering experiments. The inelastic component shown in the figure is due to both, the protein lysozyme (about 40% of the intensity of this component) and the solvent D_2O (about 60%). The structure factors obtained by integration of such spectra over the energy transfer, after subtraction of the spectral contribution due to the solvent, are the data presented in Fig. 8b. The difference (open triangles in the same figure) between integrated and elastic structure factors is small and shows no

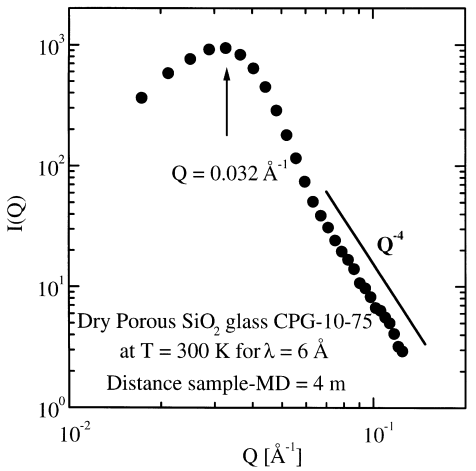

Fig. 7. Elastic structure factor of the nanoporous glass CPG-10-75, measured with $\lambda = 6$ Å with the NEAT multidetector at 4 m from the sample. The correlation peak at $Q = 0.032$ Å^{-1} and the Q^{-4} power law at higher Q values are very well observed, in agreement with the literature [28]. Illuminated sample size: 10 mm diameter. Measurement time: 3.3 h.

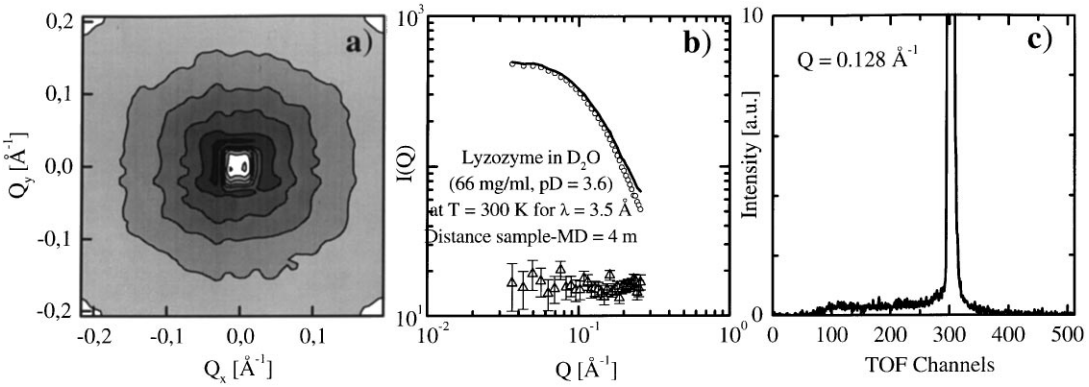

Fig. 8. (a) Diffraction pattern of a solution of lysozyme in D_2O (66 mg/ml, $pD = 3.6$) at room temperature, measured with the NEAT MD at 4 m, using $\lambda = 3.5$ Å (TOF-channels integrated). (b) Structure factors of lysozyme in solution which were inferred from (a) after subtraction of the pure D_2O contribution: The (energy-)integrated structure factor corresponding to the conventional small-angle scattering result is shown as a continuous line. Its elastic and inelastic components are represented by open circles and open triangles, respectively. (c) Inelastic small-angle scattering spectrum of the solution at $Q = 0.128$ Å^{-1}, allowing a separation of the narrow elastic from the broad inelastic scattering component. Illuminated sample size: (15 wide × 30 high) mm^2. Measurement time: 22.3 h.

Q-dependence within the limits of statistical error. This is due to the fact, that in the case of the system under study, most of these inelastic contributions stem from small-amplitude molecular motions in the protein, seen at relatively large energy transfers and correspondingly large momentum transfers Q (although measured at small scattering angles). Exciting results from inelastic scattering at small angles are expected in future studies of large-amplitude motions in biological macromolecules exhibiting for instance function-relevant hinge-bending modes, or in investigations in the context of protein unfolding. Together with the analysis of the quasielastic and inelastic SD spectra recorded at much larger angles, this should become a very powerful method to connect directly the structural information to the dynamical behaviour. This is of growing interest, in particular in disordered crystals and glasses, in soft matter physics and in biology.

7. Conclusion

One of the most important features of the time-of-flight spectrometer NEAT is its capacity of varying the energy resolution continuously over four orders of magnitude. In the case of systems exhibiting the very wide ranges of relaxation times typical, for instance, of soft and biological matter, such a capacity is definitely needed, if progress is to be made in understanding their dynamical structures. The result from purple membrane studies shown above is just one possible example demonstrating the power of this instrument for revealing the phenomenology as a first step towards unraveling the underlying fundamental characteristics of such systems. The multidetector of NEAT, with the high resolution it offers in Q and ω, is an important asset further extending the resolution capacity of the instrument, especially for single-crystal studies at large angles, but also for inelastic small-angle scattering experiments. As important complementary techniques available on the same instrument, we have also presented small- and large-angle time-of-flight diffraction. It is quite evident, that any dynamical study requires the corresponding information on the static structure of the same compound. Since in the study of soft and biological matter, and in many investigations of disordered systems in general, the exact reproducibility of the samples (for instance regarding humidity, pH, impurities, recrystallisation, etc.) is not easily garantied, the possibility of determining or verifying the structure in situ, i.e. simultaneously or immediately before or after the dynamical experiment, under identical conditions, should be extremely welcome to the experimentalist. We have demonstrated the feasibility of such experiments with a few typical examples.

Acknowledgements

Thanks are due to B. Urban and G. Steiner for valuable technical support during the experiments, and to Prof. F. Mezei for the support he gave for the continuous instrument development work. We are grateful to P. Allenspach for providing the muscovite sample, to E. Hoinkis for the CPG-10-75 specimen and to S. Dante for preparing the lysozyme solution.

References

[1] R.E. Lechner, in: M. Misawa, M. Furusaka, H. Ikeda, N. Watanabe (Eds.), Proceedings ICANS-XI, KEK Report 90-25, National Laboratory for High Energy Physics, Tsukuba, 1991, p. 717.
[2] R.E. Lechner, Neutron Scattering in the Nineties, IAEA, Vienna, 1985, p. 401.
[3] R.E. Lechner, Neutron News 7 (4) (1996) 9.
[4] R.E. Lechner, R. Melzer, J. Fitter, Physica B 226 (1996) 86.
[5] D. Wilmer, R.D. Banhatti, J. Fitter, K. Funke, M. Jansen, G. Korus, R.E. Lechner, in: T. Ramanarayanan et al. (Eds.), Ionic and Mixed Conducting Ceramics/1997, PV 97-24, The Electrochemical Society Proceedings Series, Pennington, NJ, 1997, p. 797.
[6] D. Wilmer, R.D. Banhatti, J. Fitter, K. Funke, M. Jansen, G. Korus, R.E. Lechner, Physica B 241–243 (1998) 338.
[7] D. Wilmer, K. Funke, M. Witschas, R.D. Banhatti, M. Jansen, G. Korus, J. Fitter, R.E. Lechner, Physica B 266 (1999) 60.
[8] A. Matic, J. Swenson, L. Börjesson, S. Longeville, R.E. Lechner, W.S. Howells, T. Akai, S.W. Martin, Physica B 266 (1999) 69.
[9] M. Russina, F. Mezei, W. Miekeley, W. Rönnfeld, R.E. Lechner, Physica B 234–236 (1997) 421.

[10] M. Russina, F. Mezei, in: M.R. Johnson, G.J. Kearley, H.G. Büttner (Eds.), CP479 Neutrons and Numerical Methods – N_2M, The American Institut of Physics, New York, 1999, p. 47.
[11] F. Mezei, M. Russina, J. Phys.: Condens. Matter 11 (1999) A341.
[12] F. Aliotta, M.E. Fontanella, R.E. Lechner, M. Pieruccini, B. Rufflé, C. Vasi, Phys. Rev. E 60 (1999) 7131.
[13] J. Fitter, R.E. Lechner, N.A. Dencher, in: S. Cusack, H.G. Büttner, M. Ferrand, P. Langan, P. Timmins (Eds.), Biological Macromolecular Dynamics, Proceedings of a Workshop on Inelastic and Quasielastic Neutron Scattering in Biology, Adenine Press, 1997, p. 123.
[14] J. Fitter, R.E. Lechner, N.A. Dencher, Biophys. J. 73 (1997) 2126.
[15] J. Fitter, O.P. Ernst, T. Hauß, R.E. Lechner, K.P. Hofmann, N.A. Dencher, Eur. Biophys. J. 27 (1998) 638.
[16] J. Fitter, S.A.W. Verclas, R.E. Lechner, H. Seelert, N.A. Dencher, FEBS Lett. 433 (1998) 321.
[17] J. Fitter, S.A.W. Verclas, R.E. Lechner, G. Büldt, O.P. Ernst, K.P. Hofmann, N.A. Dencher, Physica B 266 (1999) 35.
[18] M. Roepke, E. Holland-Moritz, G. Coddens, J. Fitter, R.E. Lechner, Physica B 234–236 (1997) 723.
[19] M. Roepke, E. Holland-Moritz, R. Müller, G. Coddens, R.E. Lechner, S. Longeville, J. Fitter, J. Phys. Chem. Solids 59 (1998) 2233.
[20] M. Roepke, E. Holland-Moritz, B. Büchner, H. Berg, R.E. Lechner, S. Longeville, J. Fitter, R. Kahn, G. Coddens, M. Ferrand, Phys. Rev. B 60 (1999) 9793.
[21] J. Fitter, R.E. Lechner, unpublished results.
[22] R.D. Lowde, Acta. Crystallogr. 9 (1956) 151.
[23] B. Buras, J. Leciejewicz, W. Nitc, I. Sosnowska, J. Sosnowski, F. Shapiro, Nukleonika 7–8 (1964) 523.
[24] C.J. Carlile, M.A. Adams, Physica B 182 (1992) 431.
[25] R.E. Lechner, J. Fitter, N.A. Dencher, T. Hauß, J. Mol. Biol. 277 (1998) 593.
[26] J. Ollivier, B. Rufflé, S. Longeville, P. Bourges, R.E. Lechner, B. Toudic, Europhys. Lett. (2000), in preparation.
[27] J. Ollivier, J. Etrillard, B. Toudic, C. Ecolivet, P. Bourges, A.P. Levanyuk, Phys. Rev. Lett. 81 (1998) 3667.
[28] E. Hoinkis, Adv. Colloids Interface Sci. 76–77 (1998) 39.